

Exploring the bulk of tidal charged micro-black holes

Roberto Casadio^{a*} and Octavian Micu^{b†}

^a*Dipartimento di Fisica, Università di Bologna and I.N.F.N., Sezione di Bologna,
via Irnerio 46, I-40126 Bologna, Italy*

^b*Fakultät für Physik, Technische Universität Dortmund,
D-44221 Dortmund, Germany*

Preprint number: DO-TH-10/02

Abstract

We study the bulk corresponding to tidal charged brane-world black holes. We employ a propagating algorithm which makes use of the three-dimensional multipole expansion and analytically yields the metric elements as functions of the five-dimensional coordinates and of the ADM mass, tidal charge and brane tension. Since the projected brane equations cannot determine how the charge depends on the mass, our main purpose is to select the combinations of these parameters for which black holes of microscopic size possess a regular bulk. Our results could in particular be relevant for a better understanding of TeV-scale black holes.

PACS - 04.50.Gh, 04.25.dg

1 Introduction

Several models with extra spatial dimensions [1, 2] are nowadays available, in which Standard Model fields are confined to a four-dimensional (thin) hypersurface (the brane) embedded in the higher-dimensional space-time (the bulk). The existence of extra dimensions and a sufficiently small fundamental scale of gravity would then allow for the possibility to produce microscopic black holes [3, 4, 5, 6] at the Large Hadron Collider (LHC).

In this paper we shall, in particular, consider the Randall-Sundrum (RS) brane-world of Ref. [2]. Our world is thus a three-brane (with coordinates x^i , $i, j = 0, \dots, 3$) embedded in a five-dimensional bulk with the metric

$$ds^2 = e^{-\sigma|z|} g_{ij} dx^i dx^j + dz^2, \quad (1.1)$$

where z runs along the fifth dimension and σ^{-1} is a length determined by the brane tension. This parameter relates the four-dimensional Planck mass M_p to the five-dimensional gravitational mass $M_{(5)}$ and one can have $M_{(5)} \simeq 1 \text{ TeV}/c^2$ (for bounds on σ , see, e.g., Ref. [7]) and black holes with

*E-mail: casadio@bo.infn.it

†E-mail: octavian.micu@tu-dortmund.de

mass in the TeV range. Note that, experimental limits require $M_{(5)} \gtrsim 1$ TeV, but there is no strong theoretical evidence that places $M_{(5)}$ at any specific value below M_p . The brane must also have a thickness, which we denote by L , below which deviations from the four-dimensional Newton law occur. Current precision experiments require that $L \lesssim 44 \mu\text{m}$ [8], whereas theoretical reasons imply that $L \gtrsim \ell_{(5)} \simeq \ell_p M_p/M_{(5)} \simeq 2 \cdot 10^{-19}$ m. In this context, compact sources on the brane, such as stars and black holes, have been investigated extensively. However, their description has proven rather complicated and there is little hope to obtain analytic solutions such as those found with one dimension less [9]. The present literature does in fact provide solutions on the brane [10, 11, 12], perturbative results over the RS background [13, 14] and numerical treatments [15]. (For recent reviews, see Refs. [5, 16].)

In this paper we investigate the bulk for the specific family of asymptotically flat, static and spherically symmetric solutions on the brane found in Ref. [10]. These metrics, besides the Adler-Deser-Misner (ADM) mass M , depend on an apparently free extra parameter, the so called tidal charge q . Our main aim is thus to restrict q by requiring the bulk be “regular”, meaning that it can only contain the compact extension of the brane horizon and no signs of other real singularities corresponding to physical sources extending off-brane. The method we shall use was introduced in Ref. [17] and will be briefly reviewed in the next Section, along with the results previously obtained for candidate black holes of astrophysical size. In Section 3, we shall then apply the method to the case of microscopic black holes. Regular bulks will then be obtained only for a tidal charge larger than the ADM mass but smaller than the (inverse of the) brane tension. Incidentally, this picture is compatible with the phenomenologically allowed cases, as per the analysis of Ref. [18].

We set the brane cosmological constant to zero by fine tuning the bulk cosmological constant Λ to the brane tension σ , i.e. $\Lambda = -4\sigma^2$ [2, 19] and use units with $1 = c = \hbar = M_p \ell_p = \ell_{(5)} M_{(5)}$, where $M_p \simeq 2.2 \cdot 10^{-8}$ kg and $\ell_p \simeq 1.6 \cdot 10^{-35}$ m are the Planck mass and length related to the four-dimensional Newton constant $G_N = \ell_p/M_p$. In our analysis we shall consider only the five-dimensional RS scenario with $M_{(5)} \simeq M_{ew} \simeq 1$ TeV ($\simeq 1.8 \cdot 10^{-24}$ kg), the electro-weak scale, corresponding to the length $\ell_{(5)} \simeq 2.0 \cdot 10^{-19}$ m.

2 Reconstructing the bulk

We start by reviewing the algorithm introduced in Ref. [17]. On projecting the five-dimensional vacuum Einstein equations ${}^{(5)}R_{\mu\nu} = \Lambda g_{\mu\nu} = -4\sigma^2 g_{\mu\nu}$ (with $\mu, \nu = 0, \dots, 4$) onto the brane and introducing Gaussian normal coordinates x^i and z ($z = 0$ on the brane), one obtains the constraints

$${}^{(5)}R_{iz} \Big|_{z=0} = {}^{(4)}R \Big|_{z=0} = 0, \quad (2.1)$$

where ${}^{(4)}R$ is the four-dimensional Ricci scalar and use has been made of the necessary junction equations [20]. Eqs. (2.1) are analogous to the momentum and Hamiltonian constraints in the ADM decomposition and select admissible field configurations along a given hypersurface of constant z . Acceptable configurations are then “propagated” off-brane by the remaining Einstein equations,

$${}^{(5)}R_{ij} = -4\sigma^2 g_{ij}. \quad (2.2)$$

The above “Hamiltonian” constraint is weaker than the purely four-dimensional vacuum equations $R_{ij} = 0$, being equivalent to $R_{ij} = E_{ij}$, where E_{ij} is (proportional to) the (traceless) projection of

the five-dimensional Weyl tensor on the brane [19]. We then consider five-dimensional metrics of the form (1.1) with

$$ds_{(4)}^2 \equiv e^{-\sigma|z|} g_{ij} dx^i dx^j = -N(r, z) dt^2 + A(r, z) dr^2 + R^2(r, z) d\Omega^2 , \quad (2.3)$$

where $d\Omega^2 \equiv d\theta^2 + \sin^2 \theta d\phi^2$ and N , A and R are functions to be determined. The momentum constraint is then identically solved and the ‘‘Hamiltonian’’ constraint reads

$$2 \left(\frac{N'_B}{N_B} \right)' + \left(\frac{N'_B}{N_B} + \frac{4}{r} \right) \left(\frac{N'_B}{N_B} - \frac{A'_B}{A_B} \right) = \frac{4}{r^2} (A_B - 1) , \quad (2.4)$$

where the subscript B means that all functions are evaluated on the brane at $z = 0$, $' \equiv \partial/\partial r$ and we set $R_B = r$ thanks to (four-dimensional) spherical symmetry [21].

2.1 Propagating algorithm

The bulk metric will be determined in three steps:

1. choose a metric of the form (2.3) whose projection on the brane,

$$ds_{(4)}^2 \Big|_{z=0} = -N_B(r) dt^2 + A_B(r) dr^2 + r^2 d\Omega^2 , \quad (2.5)$$

solves the constraint (2.4);

2. expand this metric in powers of $1/r$ (four-dimensional *multipole expansion*) to order n ,

$$\left. \begin{array}{l} N_n(r, z) \\ A_n(r, z) \\ R_n^2(r, z) \end{array} \right\} \equiv \sum_{k=0}^n \frac{1}{r^k} \left\{ \begin{array}{l} n_k(z) \\ a_k(z) \\ r^2 c_k(z) \end{array} \right. , \quad (2.6)$$

where $n_k(0)$, $a_k(0)$ and $c_k(0)$ reproduce the solution chosen at step 1 (to order n):

$$\sum_{k=0}^n \frac{1}{r^k} \left\{ \begin{array}{l} n_k(0) \\ a_k(0) \\ r^2 c_k(0) \end{array} \right\} = \left\{ \begin{array}{l} N_B(r) \\ A_B(r) \\ r^2 \end{array} \right\} + \mathcal{O} \left(\frac{1}{r^{n+1}} \right) ; \quad (2.7)$$

3. substitute the sum (2.6) into Eq. (2.2) and integrate analytically in z the (three) equations thus obtained for the functions $n_n(z)$, $a_n(z)$ and $c_n(z)$.

This procedure turns out to be particularly convenient because it converts the Einstein equations (2.2) into second order ordinary differential equations of the form

$$\frac{d^2 f_n}{dz^2} - \sigma^2 f_n = F_{k < n} , \quad (2.8)$$

where f_n is any of the functions $n_n(z)$, $a_n(z)$ and $c_n(z)$ ($n \geq 1$), and $F_{k < n}(z)$ a functional of the lower order terms $f_{k < n}$'s and their first and second derivatives. The relevant boundary conditions are given by Eq. (2.7) for $f_n(0)$ and the junction conditions [20]

$$\frac{df_n}{dz} \Big|_{z=0} = -\sigma f_n(0) . \quad (2.9)$$

For $n = 0$ one has a system of three coupled second order ordinary differential equations for the f_0 's and the corresponding Cauchy problem is uniquely solved by the usual warp factor, $f_0 = \exp(-\sigma z)$. The $F_{k < n}$'s then turn out to be such that the Cauchy problem at order n admits analytical solutions and one can determine the functions f_n recursively.

Except for the algebraic constraints following from Eq. (2.4), the coefficients $n_k(0)$ and $a_k(0)$, which are related to the shape of the source, can be chosen at will. However, it is in general difficult to pinpoint one parameter (among the coefficients of the multipole expansion) whose ‘‘smallness’’ guarantees that orders higher than n be negligible. Ideally, the resulting bulk metric is reliable for those values of r and z such that

$$\frac{|f_{n+1}(z)|}{r^{n+1}} \ll \left| \sum_{k=0}^n \frac{f_k(z)}{r^k} \right|, \quad (2.10)$$

for given values of the parameters $n_k(0)$ and $a_k(0)$. In general, for a given z , such a condition will only be satisfied for sufficiently large r . This implies that different choices of $n_k(0)$ and $a_k(0)$ might lead to bulk space-times which remain indistinguishable because the differences are confined within too small a region close to $r = z = 0$. Conversely, by looking at the bulk metric in our approach, we may not be able to distinguish the correct brane source from other sources, e.g., those which spread slightly into the bulk.

2.2 Astrophysical examples

As examples of brane metrics, Ref. [17] considered the solutions given in Refs. [10, 11, 12] which can be expressed in terms of the ADM mass $M = r_h/2$ (r_h is the event horizon) and the post-Newtonian parameters $\beta = \gamma = 1 + \frac{1}{3}\eta$ [22] on the brane. Exact Schwarzschild on the brane, $\eta = 0$, is called black string (BS) [23] and suffers of serious stability problems [23, 24]. One can therefore argue that brane-world black holes have $\eta \neq 0$ and cases with $\eta < 0$ are favored, since $\eta > 0$ implies anti-gravity effects [12]. For astrophysical sources of solar mass size, Ref. [17] made use of the typical values $M = 10^7 \sigma^{-1} \sim 1 \text{ km}$ and $\eta = -10^{-4}$. In such a range,

$$M \sigma \gg 1, \quad (2.11)$$

(with $|\eta| \ll 1$), one finds a qualitatively identical behavior for all brane metrics in Refs. [10, 11, 12]. In particular, positive exponentials appear in the metric functions, which are non-perturbative in z , and make the expansion in $1/r$ preferable (or complementary) to the expansion for small z .

For $\eta < 0$, it was found that, for $n \geq 3$ and $r > 0$, there exists a $z = z_n^{\text{axis}}(r)$ such that $R_n^2(r, z_n^{\text{axis}}) = 0$. Since $4\pi R^2$ is the proper area of the sphere $t = r = z = \text{constant}$, this suggests that the axis of cylindrical symmetry is given by a line $z = z^{\text{axis}}(r)$. Although the condition (2.10) fails for $z = z_n^{\text{axis}}$, in the physically interesting range, the $1/r$ expansion yields rather stable values of z_n^{axis} in a wide span of n , stability improves for larger values of r and becomes very satisfactory for $r \gtrsim r_h$. For example, for $r \gg r_h$, one finds

$$z_5^{\text{axis}} \simeq \frac{1}{2\sigma} \ln \left(\frac{3\sigma^2 r^3}{-\eta M} \right), \quad (2.12)$$

which numerically agrees fairly well with $z_{5 < n \leq 19}^{\text{axis}}$. If the horizon closes in the bulk, then it must cross the axis of cylindrical symmetry at a point (the ‘‘tip’’) of finite coordinates $(r^{\text{tip}}, z^{\text{tip}})$, which can be obtained approximately by solving

$$N_n(r_n^{\text{tip}}, z_n^{\text{tip}}) = R_n^2(r_n^{\text{tip}}, z_n^{\text{tip}}) = 0. \quad (2.13)$$

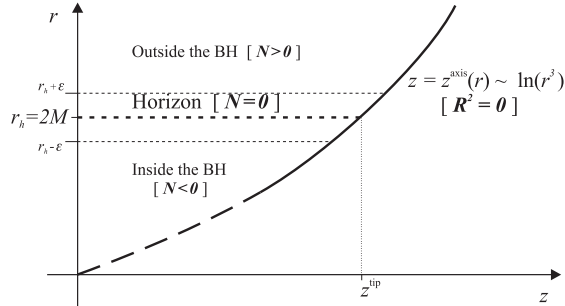


Figure 1: Qualitative picture of bulk structure.

For $n = 5$, one finds

$$z_5^{\text{tip}} \simeq \frac{1}{\sigma} \ln \left(\frac{M \sigma}{\sqrt{-\eta}} \right). \quad (2.14)$$

For large values of n , one can only solve Eqs. (2.13) numerically and finds a good parameterization for the horizon is given by $r \simeq r_h$ and $0 \leq z \lesssim z^{\text{axis}}(r_h) \simeq z^{\text{tip}}$ (see Fig. 1), which strongly suggests that the horizon closes in the bulk, in accord with numerical analysis [15]. One can also estimate how flattened the horizon is towards the brane by comparing the proper length of a circle on the brane-horizon, $\mathcal{C}_{\parallel} = 2\pi r_h$, with the length of an analogous curve perpendicular to the brane, $\mathcal{C}_{\perp} \simeq 4z^{\text{tip}}$. Since their ratio is huge, one can in fact speak of a “pancake” horizon as was suggested, e.g., in Ref. [13]. In particular, the area of the (bulk) horizon is approximately equal to the four-dimensional (brane) expression ¹,

$${}^{(5)}\mathcal{A} \simeq 4\pi \int_0^{z_5^{\text{tip}}} R^2(r_h, z) dz \simeq \frac{16\pi}{\sigma} (2M)^2, \quad (2.15)$$

where we again used $M\sigma \gg 1$. Drawing upon the above picture, in particular the crossing of lines of constant r with the axis of cylindrical symmetry at finite z , one can infer that the Kretschmann scalar in these space-times is well-behaved [17], contrary to the BS [23].

We conclude by mentioning that cases with $\eta > 0$ show a very different qualitative behavior. One finds that $R_n^2(r, z)$ is generically a (monotonically) increasing function of z for all (sufficiently large) values of r , as one would indeed expect on a negative tension brane [19]. However, for any $r_1, r_2 > 0$ there now exists $z_n^*(r_1, r_2)$ such that $R_n^2(r_1, z_n^*) = R_n^2(r_2, z_n^*)$, i.e., space-like geodesics of constant r display caustics and the Gaussian coordinates (r, z) do not cover the whole bulk [21].

3 Tidal charged black holes

We now proceed to analyze the brane metric found in Ref. [10],

$$ds_{(4)}^2 \Big|_{z=0} = -N_B dt^2 + N_B^{-1} dr^2 + r^2 d\Omega^2, \quad (3.1)$$

¹The fundamental (possibly TeV scale) five-dimensional gravitational coupling $G_{(5)} \sim G_N/\sigma$, where G_N is the four-dimensional Newton constant [2]. Thus, from (2.15), one has ${}^{(5)}\mathcal{A}/G_{(5)} \sim M^2/G_N \sim {}^{(4)}\mathcal{A}/G_N$.

with

$$N_{\text{B}} = 1 - \frac{2M}{r} - \frac{Q}{r^2}, \quad (3.2)$$

and [12]

$$\eta = -\frac{2Q}{M^2}. \quad (3.3)$$

The tidal charge Q is assumed positive, so that there is one horizon at

$$R_{\text{H}} = \left(M + \sqrt{M^2 + Q} \right). \quad (3.4)$$

Moreover, the Einstein equations projected onto the brane do not relate the ADM mass to the tidal charge, and Q therefore appears as a free parameter. We however expect that Q vanishes when M does, and the former should thus be a function of the latter [4]. Nonetheless, we shall apply our propagating algorithm to the metric (3.1) with independent M and Q .

3.1 TeV-scale black holes

Like in Refs. [4, 18, 27], we are here interested in microscopic black holes with a mass M close to the assumed value of $M_{(5)}$. Since $\sigma^{-1} \gtrsim \ell_{\text{p}}$, for such small black holes the opposite of the condition (2.11) holds, namely

$$M \sigma \ll 1. \quad (3.5)$$

The above relation allows one to constrain the relative strength of tidal effects with respect to the Newtonian potential. This kind of analysis was indeed performed earlier in Ref. [18], and we here review it briefly. First of all, we recall that Q is related to the charge q of Refs. [4, 18, 27] by

$$Q = q \ell_{\text{p}}^2 \left(\frac{M_{\text{p}}}{M_{(5)}} \right)^2 = \ell_{\text{p}}^{2-\beta} \left(\frac{M_{\text{p}}}{M_{(5)}} \right)^{\alpha+\beta+2} M^{\beta}, \quad (3.6)$$

where α and $\beta > 0$ are parameters. We then note that the tidal term in the metric dominates over the usual General Relativistic term for $r \lesssim r_{\text{c}}$, with

$$r_{\text{c}} \simeq \ell_{\text{p}}^{2-\beta} \left(\frac{M_{\text{p}}}{M_{(5)}} \right)^{\alpha+\beta+2} M^{\beta-1}. \quad (3.7)$$

This implies that r_{c} must be shorter than the length scale L above which corrections to the Newtonian potential have not yet been detected. That is, we impose

$$r_{\text{c}} \ll L, \quad (3.8)$$

and the black hole is therefore “small” provided

$$R_{\text{H}} \ll r_{\text{c}} \ll L. \quad (3.9)$$

In fact, for $R_{\text{H}} \ll r_{\text{c}}$, the horizon radius can be approximated by the tidal part of Eq. (3.4),

$$R_{\text{H}} \simeq \ell_{\text{p}}^{\frac{2-\beta}{2}} \left(\frac{M_{\text{p}}}{M_{(5)}} \right)^{\frac{\alpha+\beta+2}{2}} M^{\frac{\beta}{2}}, \quad (3.10)$$

otherwise, it approaches the usual four-dimensional expression $R_{\text{H}} \simeq 2M$. The effective four-dimensional Euclidean action [4, 26], for small black holes, can be approximated by

$$S_{(4)}^{\text{E}} = \frac{M_{\text{p}} (4\pi R_{\text{H}}^2)}{16\pi \ell_{\text{p}}} \simeq \ell_{\text{p}} M_{\text{p}} \left(\frac{M}{M_{\text{eff}}} \right)^{\beta}, \quad (3.11)$$

where

$$M_{\text{eff}} = \ell_{\text{p}} \left[\frac{1}{4} \left(\frac{M_{\text{p}}}{M_{(5)}} \right)^{\alpha+\beta+2} \right]^{-\frac{1}{\beta}}. \quad (3.12)$$

The area law then implies that the degeneracy of a black hole is counted in units of M_{eff} and a black hole is classical if its mass is much larger than M_{eff} , which implies that M_{eff} must be no larger than $M_{(5)}$ in order to have TeV-scale black holes. Since $\beta > 0$, $M_{\text{eff}} \lesssim M_{(5)}$ implies

$$\alpha \gtrsim -2, \quad (3.13)$$

for all values of β . For $\beta \neq 1$, one then has that $r_{\text{c}} = L$ corresponds to a critical mass

$$M_{\text{c}} = \left[L \ell_{\text{p}}^{\beta-2} \left(\frac{M_{\text{p}}}{M_{(5)}} \right)^{-\alpha-\beta-2} \right]^{\frac{1}{\beta-1}}. \quad (3.14)$$

Further, for $\beta \neq 2$, the condition that $r_{\text{c}} = R_{\text{H}}$ leads to

$$M \simeq M_{\text{H}} \equiv \ell_{\text{p}} \left(\frac{M_{\text{p}}}{M_{(5)}} \right)^{-\frac{\alpha+\beta+2}{\beta-2}}, \quad (3.15)$$

whereas for $\beta = 2$ is already assured by Eq. (3.13). If we look at the conditions (3.8) and (3.9) for $\beta \neq 1$ and $\beta \neq 2$, so that M_{c} and M_{H} are properly defined as above, we notice that the condition (3.8) implies

$$M^{\beta-1} \ll L \ell_{\text{p}}^{\beta-2} \left(\frac{M_{\text{p}}}{M_{(5)}} \right)^{-\alpha-\beta-2}, \quad (3.16)$$

and we have the two cases

$$M \gtrsim M_{\text{c}}, \quad \text{for } 0 < \beta < 1 \quad (3.17)$$

$$M \lesssim M_{\text{c}}, \quad \text{for } \beta > 1. \quad (3.18)$$

Similarly, one can analyze the lower bound in Eq. (3.9). Since we are only interested in small black holes, we assume that the condition (3.16) is satisfied. Below the critical radius, where the tidal term dominates, the horizon radius (3.4) can be approximated by the tidal component and $R_{\text{H}} \ll r_{\text{c}}$ yields

$$M^{\beta-2} \gg \ell_{\text{p}}^{\beta-2} \left(\frac{M_{\text{p}}}{M_{(5)}} \right)^{-\alpha-\beta-2}. \quad (3.19)$$

We again have two separate cases:

$$M \lesssim M_{\text{H}} , \quad \text{for } 0 < \beta < 2 \quad (3.20)$$

$$M \gtrsim M_{\text{H}} , \quad \text{for } \beta > 2 . \quad (3.21)$$

A detailed discussion on the constraints on the parameters α and β for small black holes can be found in Ref. [18]. The overall conclusion is that, for any positive value of the parameter β , the parameter α is constrained in the range

$$-2 \lesssim \alpha \lesssim -1.1 . \quad (3.22)$$

Finally, let us remark that the parameterization (3.6) for Q in terms of α and β is not necessary for the present investigation, and was only recalled here to establish a connection with previous results [4, 18, 27].

3.2 Analytical and numerical results

Starting from the brane metric (3.1), we ran our propagating algorithm to obtain the bulk metric with terms up to $n \leq 29$ for any M , Q and σ . These analytical expressions can then be used to study how the axis of cylindrical symmetry and the horizon (3.4) propagate into the bulk numerically. In particular, the axis of cylindrical symmetry should start on the brane at $r = z = 0$ and, in the (r, z) -plane, be again represented by the line $R^2(r, z^{\text{axis}}(r)) = 0$ to the right of which $R^2 > 0$, whereas the region to the left of $z = z^{\text{axis}}(r)$, having $R^2 < 0$, is unphysical. Analogously, a proper horizon should start from the brane horizon at $r = R_{\text{H}}$, $z = 0$ and be represented by a line $N(r, z^{\text{h}}(r)) = 0$ inside the region to the right of the axis $z = z^{\text{axis}}(r)$. As in Ref. [17], we are searching for those cases in which both the axis and the horizon are regular and the horizon closes towards the axis along the extra dimension. We shall again call the ‘‘tip’’ the point where axis and horizon cross. Existence of the tip would thus signal the fact that the real singularity is enclosed within the horizon and the corresponding brane metric is a viable candidate for a brane-world black hole.

For example, the metric elements to order $n = 5$ are simple enough for displaying, namely

$$N_5(r, z) = e^{-\sigma z} \left[1 - \frac{2M}{r} - \frac{Q}{r^2} + \frac{(e^{-\sigma z} - 1)^2 Q}{\sigma^2 r^4} - \frac{2(e^{-\sigma z} - 1)^2 Q M}{\sigma^2 r^5} \right] \quad (3.23)$$

$$A_5(r, z) = e^{-\sigma z} \left\{ 1 + \frac{2M}{r} - \frac{4M^2 + Q}{r^2} + \frac{4M(2M^2 + Q)}{r^3} + \frac{(e^{-\sigma z} - 1)^2 Q + \sigma^2(16M^4 + 12M^2Q + Q^2)}{\sigma^2 r^4} + \frac{2M[(e^{-\sigma z} - 1)^2 Q + \sigma^2(16M^4 + 16M^2Q + 3Q^2)]}{\sigma^2 r^5} \right\} \quad (3.24)$$

$$R_5^2(r, z) = r^2 e^{-\sigma z} \left[1 - \frac{(e^{-\sigma z} - 1)^2 Q}{\sigma^2 r^4} \right] . \quad (3.25)$$

From Eq. (3.25), the axis of cylindrical symmetry at order $n = 4$ is then given by

$$z_4^{\text{axis}}(r) = \frac{1}{\sigma} \ln \left(1 + \frac{\sigma r^2}{\sqrt{Q}} \right) , \quad (3.26)$$

and, analogously, from Eq. (3.23), the horizon at $n = 4$ is located at

$$z_4^{\text{h}}(r) = \frac{1}{\sigma} \ln \left(1 + \sigma r \sqrt{1 + \frac{2Mr}{Q} - \frac{r^2}{Q}} \right) . \quad (3.27)$$

Finally, the horizon intersects the axis of symmetry at

$$\begin{aligned} r_4^{\text{tip}} &= \frac{1}{2} \left(M + \sqrt{M^2 + 2Q} \right) \\ z_4^{\text{tip}} &= \frac{1}{\sigma} \ln \left[1 + \frac{\sigma}{4\sqrt{Q}} \left(M + \sqrt{M^2 + 2Q} \right)^2 \right] . \end{aligned} \quad (3.28)$$

Note that r_4^{tip} and z_4^{tip} are always real and no constraint is therefore derived for M , Q and σ at $n = 4$ from requiring the existence of a “tip”. However, looking at the term of order $n = 5$ in Eq. (3.23), one realizes that higher order terms will appear with possible alternating signs and the picture become more involved, as we are now going to show.

In fact, the propagating algorithm produces very cumbersome expressions rather quickly as one raises the order n of the multipole expansion. In order to visualize the bulk structure, it is then convenient to consider specific numerical values for the parameters M , Q and σ in the range of interest for our study. For this purpose, we also define the dimensionless quantities $\bar{Q} = Q/\ell_{\text{p}}^2$, $\bar{M} = M/\ell_{\text{p}}$ and $\bar{\sigma} = \ell_{\text{p}} \sigma$. The condition (3.5) then reads

$$\bar{M} \ll \bar{\sigma}^{-1} . \quad (3.29)$$

Further, the relation (3.6) can be rewritten as

$$\bar{Q} = \bar{M}^\beta \left(\frac{M_{\text{p}}}{M_{(5)}} \right)^{\alpha+\beta+2} . \quad (3.30)$$

where $\beta > 0$ and α satisfies Eq. (3.22). We therefore find that

$$\bar{Q} \gg \bar{M} , \quad (3.31)$$

and microscopic tidal-charged black holes should look very similar to five-dimensional Schwarzschild black holes, in agreement with perturbative calculations [13].

From the metric elements evaluated to order $n = 29$, we found that the horizon is well-behaved and the bulk is regular provided

$$\bar{M} \lesssim \bar{Q} \ll \bar{\sigma}^{-1} . \quad (3.32)$$

whereas the bulk shows some pathological behaviors when one of the conditions in Eq. (3.32) fails, namely for $\bar{Q} < \bar{M}$ or $\bar{\sigma}^{-1} < \bar{Q}$. Note that Eq. (3.32) implies both (3.29) and (3.31), but the latter is required *a priori*, in order to have small black holes (not for regularity purposes).

\bar{M}	\bar{Q}	10	1	10^{-1}	10^{-2}	10^{-3}	10^{-4}	10^{-5}
10^{-1}		MsA MH	MsA OH	MH	MsA MH	MsA MH	MsA MH	MsA MH
10^{-2}		MsA OH	MsA OH	MH	OH	MH	MsA MH	MsA MH
10^{-3}		MsA MH	MsA MH	R	R	MIA	OH	MH
10^{-4}		MsA OH	MsA MH	R	R	R	R	MIA OH
10^{-5}		OH	MH	R	R	R	R	MIA OH

Table 1: Bulk pathologies (or absence thereof).

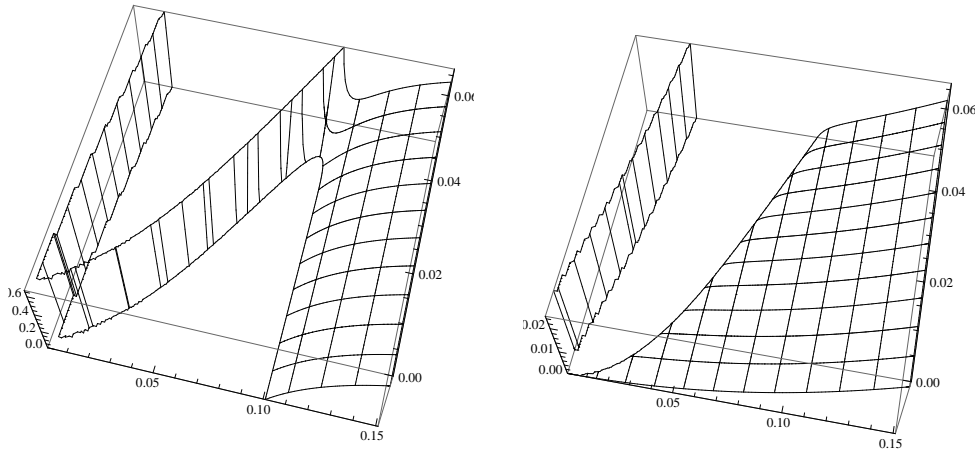


Figure 2: Left panel: Plot of $N = -g_{tt}(r, z) \geq 0$. Horizon is line $N = 0$. Right panel: Plot of $R^2(r, z) \geq 0$. Axis of cylindrical symmetry is line $R^2 = 0$ right of which $R^2 > 0$ and space to left of axis ($R^2 < 0$) is unphysical. (We set $\bar{\sigma} = 1$, $\bar{M} = 10^{-3}$ and $\bar{Q} = 10^{-2}$)

The above result was obtained by performing an extended survey in the space of the parameters \bar{M} and \bar{Q} with $\bar{\sigma}^{-1} = 1$. A sample is shown in Table 1, where the entries represent the peculiar features of each case, which we describe in details below. Before that, we remark that we were not able to establish a one-to-one correspondence between Q and M , but we rather obtained a range of possible values for Q given a value of M . This is a consequence of the multipole expansion: the cases with regular bulk (labelled as R in Table 1) for a given value of M represent different brane metrics whose bulks do not show any pathology within the level of precision allowed by our method. In particular, we expect each value of Q corresponds to a different shape of the source, but when the sources are localized very near $r = z = 0$, the multipole expansion cannot discern them and we are therefore not able to rule out cases for which, e.g., the source spreads off-brane and is not point-like.

3.2.1 Regular bulk (R)

We denote with R the good candidates which show no pathology. An example is given in Figs. 2-3 for $\bar{\sigma} = 1$, $\bar{M} = 10^{-3}$ and $\bar{Q} = 10^{-2}$. From the left panel in Fig. 2, we see a horizon at $r \simeq 0.1$ on the brane which closes towards smaller values of r in the bulk. The right panel shows R^2 plotted in

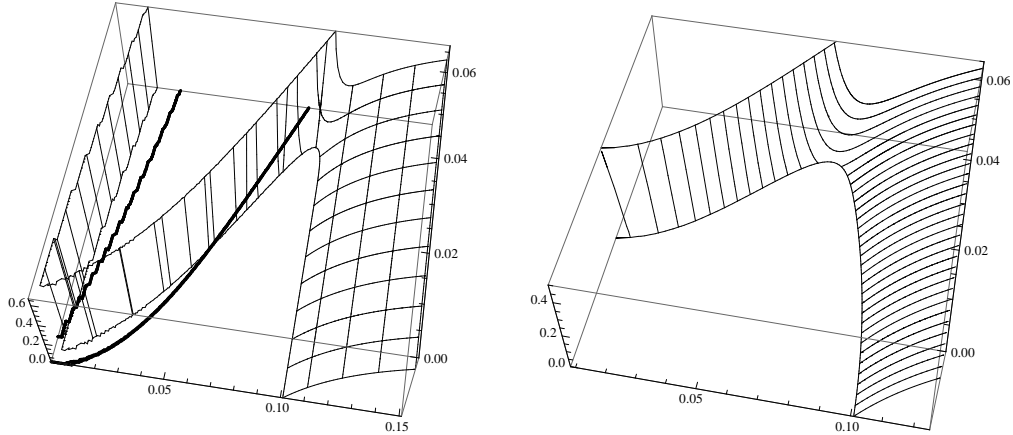


Figure 3: Left panel: Plot of $N = -g_{tt}(r, z)$ and $R^2(r, z) = 0$ (thick line) from Fig. 2. Right panel: Plot of $N = -g_{tt}(R, z) \geq 0$. Horizon is at $N = 0$ and axis of cylindrical symmetry at $R = 0$. (We set $\bar{\sigma} = 1$, $\bar{M} = 10^{-3}$ and $\bar{Q} = 10^{-2}$)

the (r, z) -plane as well. The space to the left of the line where $R^2 = 0$ is unphysical. As mentioned before, for the horizon to close in the bulk, it must cross the axis of cylindrical symmetry at a tip point, where $R^2 = 0$. The left panel in Fig. 3 shows that there is indeed such a point. Finally, the right panel in Fig. 3 displays N directly as a function of (R, z) and shows that the horizon approaches the axis where $R = 0$.

A final remark is in order. Some of the plots for regular cases show an axis that does not exactly start from $r = z = 0$. This can be due to the limitations of the multipole expansion and necessarily limited numerical precision. We therefore do not consider this feature as evidence of any pathologies.

3.2.2 Multiple axis (MsA and MIA)

There are cases which show more, apparently disconnected, lines $z = z^{\text{axis}}(r)$ along which $R^2 = 0$, as shown by the two examples given in Fig. 4. In the left panel, we see a first line $z = z^{\text{axis}}(r)$ close to the left bottom corner, and what looks like a larger copy of it still emanating from $r = 0$. In this case, it is difficult to assess whether the two lines are disconnected or rather meet around $r = 0$, since the multipole expansion is not reliable for small r . We denote this first case as Multiple short Axis (MsA). In the right panel, we see a similar $z = z^{\text{axis}}(r)$ near the bottom left corner which winds around $r = z = 0$, and a second, V-shaped $z = z^{\text{axis}}(r)$ in the right top corner. These two lines appear clearly disconnected and the larger one is well separated from the brane axis at $r = z = 0$. We denote this case as Multiple large Axis (MIA).

In general, we consider the presence of a multiple axis of the first kind (MsA) as a warning sign that our approach might not be able to describe the space-time reliably around the axis. However, a multiple axis of the second kind (MIA) makes the bulk irregular and unacceptable.

3.2.3 Multiple horizon (MH)

With Multiple Horizon (MH) we denote cases in which there are more lines $z = z^{\text{h}}(r)$ in the region where $R^2 > 0$. We consider the appearance of any $z = z^{\text{h}}(r)$, beside the one generating from

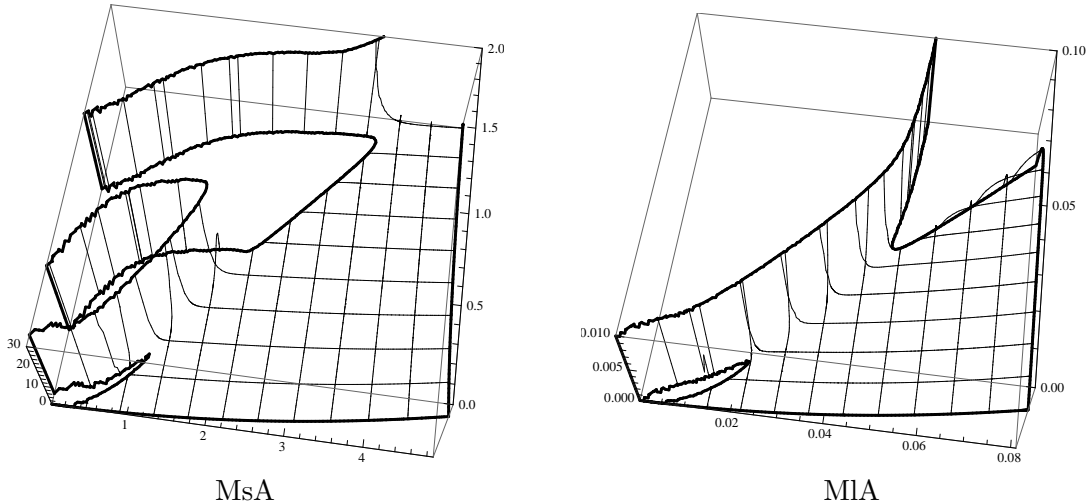


Figure 4: Left panel: Plot of $R^2(r, z) \geq 0$ for $\bar{M} = 10^{-1}$ and $\bar{Q} = 10$. One axis is in bottom left corner and one above it. Right panel: Plot of $R^2(r, z) \geq 0$ for $\bar{M} = \bar{Q} = 10^{-3}$. One axis is in the left bottom corner and one appears in the top right. (We set $\bar{\sigma} = 1$.)

$r = R_H$, as a sufficient reason to discard the case. Ideally, such situations should contain extra sources beside the point-like tidal black hole. An example is given in the left panel of Fig. 5. Near the left bottom corner, we see the brane horizon which closes towards the axis as in the regular cases. However, a second horizon appears in the bulk, near the right top corner, where $R^2 > 0$.

3.2.4 Open horizon (OH)

When the horizon starting from $r = R_H$ at $z = 0$ does not close towards the axis, we have an Open Horizon (OH). This is again considered a sufficient reason to discard the case, since it presumably signal the source at $r = z = 0$ is not point-like but extends off-brane, or other off-brane sources are anyway present. An example of this behavior is shown in the right panel of Fig. 5.

4 Conclusions

In this paper, we studied the bulk corresponding to tidal charged brane-world black holes for the case of microscopic masses within the energy range of the LHC. Such black holes are characterized by the four-dimensional ADM mass \bar{M} and tidal charge \bar{Q} [10]. To these (dimensionless) parameters, one must also add the brane density $\bar{\sigma}$, and the conditions for black holes to be in the TeV-range are then given in Eqs. (3.29) and (3.31).

In order to reconstruct the bulk, we employed a propagating algorithm which makes use of the three-dimensional multipole expansion of any brane metric of choice, and then allows one to determine analytically the corresponding five-dimensional metric elements. Given a generic brane-world metric, it is possible that singularities of various kind appear off the brane, thus signaling that the starting four-dimensional metric is not a good candidate in RS. For the specific family of brane-world metrics of interest here, we found that the bulk structure is regular for \bar{M} , \bar{Q} and $\bar{\sigma}^{-1}$ satisfying Eq. (3.32). By regular we mean that the brane-world horizon is propagated into the bulk smoothly and closes towards the axis of cylindrical symmetry along the extra dimension for

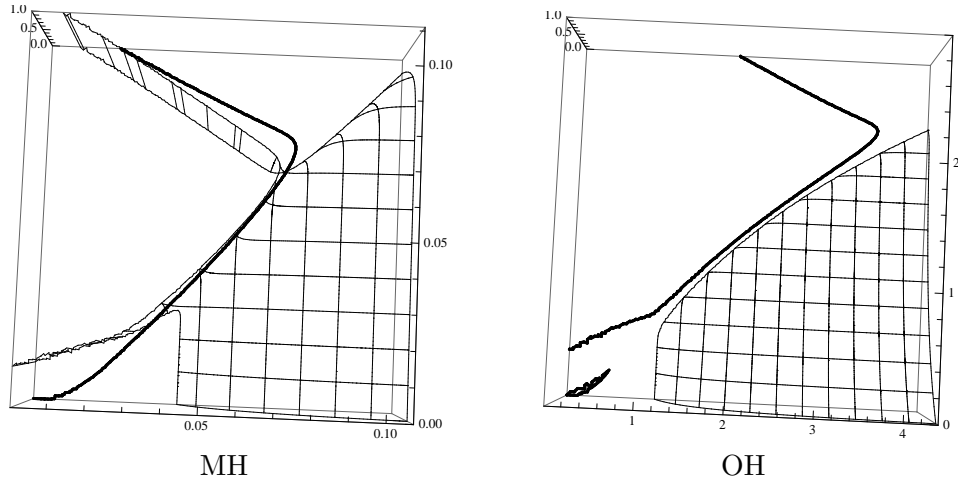


Figure 5: Left panel: Plot of $N = -g_{tt}(r, z) \geq 0$ and $R^2(r, z) = 0$ (thick line) for $\bar{M} = 10^{-2}$ and $\bar{Q} = 10^{-3}$. Horizon generating from brane is near bottom left corner and crosses axis. Second horizon appears near right top corner starting from axis. Right panel: Plot of $N = -g_{tt}(r, z) \geq 0$ and $R^2(r, z) = 0$ (thick line) for $\bar{M} = 10^{-1}$ and $\bar{Q} = 1$. Horizon starts from brane and never crosses axis. (We set $\bar{\sigma} = 1$)

$\bar{M} \lesssim \bar{Q} \ll \bar{\sigma}^{-1}$ [see Section 3.2.1]. On the contrary, when any of these conditions (3.32) is violated [keeping Eq. (3.31) in order for the black hole to be small], the bulk shows very peculiar causal structures described in Sections 3.2.2-3.2.4.

By comparing this result with the form of the tidal charge (3.6) first given in Ref. [18], we found that the values of the parameters α and β which ensure (3.32) are indeed the same that were previously selected in Ref. [18] on purely phenomenological grounds. We wish to stress, nonetheless, that the results presented here do not depend on the specific form chosen to relate Q to M and other parameters in the model, since they were all kept free when generating the bulk metric.

Acknowledgments

We thank B. Harms for stimulating discussions. R.C. is supported by INFN grant BO11.

References

- [1] N. Arkani-Hamed, S. Dimopoulos and G.R. Dvali, Phys. Lett. B **429**, 263 (1998); Phys. Rev. D **59**, 086004 (1999); I. Antoniadis, N. Arkani-Hamed, S. Dimopoulos and G.R. Dvali, Phys. Lett. B **436**, 257 (1998); L. Randall and R. Sundrum, Phys. Rev. Lett. **83**, 3370 (1999).
- [2] L. Randall and R. Sundrum, Phys. Rev. Lett. **83**, 4690 (1999).
- [3] P.C. Argyres, S. Dimopoulos and J. March-Russell, Phys. Lett. B **441**, 96 (1998); S. Dimopoulos and G.L. Landsberg, Phys. Rev. Lett. **87**, 161602 (2001); S.B. Giddings and S. D. Thomas, Phys. Rev. D **65**, 056010 (2002). C.M. Harris, P. Richardson and B.R. Webber, JHEP **0308**, 033 (2003); G.L. Alberghi, R. Casadio and A. Tronconi, J. Phys. G **34**, 767 (2007); M. Cavaglia,

- R. Godang, L. Cremaldi and D. Summers, *Comput. Phys. Commun.* **177**, 506 (2007); D.C. Dai et al., *Phys. Rev. D* **77**, 076007 (2008); J.A. Frost et al., *JHEP* **0910**, 014 (2009); T. Burschil and B. Koch, “Renormalization group improved black hole space-time in large extra dimensions,” arXiv:0912.4517 [hep-ph]; D.M. Gingrich, “Monte Carlo event generator for quantum black hole production and decay in proton-proton collisions,” arXiv:0911.5370 [hep-ph];
- [4] R. Casadio and B. Harms, *Int. J. Mod. Phys. A* **17**, 4635 (2002).
- [5] M. Cavaglia, *Int. J. Mod. Phys. A* **18**, 1843 (2003); P. Kanti, *Int. J. Mod. Phys. A* **19**, 4899 (2004).
- [6] D.M. Gingrich, “Production of tidal-charged black holes at the Large Hadron Collider,” arXiv:1001.0626.
- [7] C.G. Boehmer, T. Harko and F.S.N. Lobo, *Class. Quant. Grav.* **25**, 045015 (2008).
- [8] D.J. Kapner et al., *Phys. Rev. Lett.* **98**, 021101 (2007).
- [9] R. Emparan, G. T. Horowitz and R. C. Myers, *JHEP* **0001** (2000) 007.
- [10] N. Dadhich, R. Maartens, P. Papadopoulos and V. Rezanian, *Phys. Lett. B* **487** (2000) 1.
- [11] C. Germani and R. Maartens, *Phys. Rev. D* **64** (2001) 124010; R. Casadio and C. Germani, *Prog. Theor. Phys.* **114** (2005) 23.
- [12] R. Casadio, A. Fabbri and L. Mazzacurati, *Phys. Rev. D* **65** (2002) 084040.
- [13] S.B. Giddings, E. Katz and L. Randall, *JHEP* **0003** (2000) 023.
- [14] J. Garriga and T. Tanaka, *Phys. Rev. Lett.* **84** (2000) 2778.
- [15] A. Chamblin, H.S. Reall, H.a. Shinkai and T. Shiromizu, *Phys. Rev. D* **63** (2001) 064015; T. Wiseman, *Phys. Rev. D* **65** (2002) 124007.
- [16] P. Kanti, *J. Phys. Conf. Ser.* **189**, 012020 (2009); R. Whisker, “Braneworld Black Holes,” arXiv:0810.1534 [gr-qc]; R. Gregory, *Lect. Notes Phys.* **769** (2009) 259.
- [17] R. Casadio and L. Mazzacurati, *Mod. Phys. Lett. A* **18** (2003) 651.
- [18] R. Casadio, S. Fabi, B. Harms and O. Micu, “Theoretical survey of tidal-charged black holes at the LHC,” arXiv:0911.1884 [hep-th].
- [19] T. Shiromizu, K.i. Maeda and M. Sasaki, *Phys. Rev. D* **62** (2000) 024012.
- [20] W. Israel, *Nuovo Cim. B* **44S10** (1966) 1 [Erratum-ibid. *B* **48** (1967) NUCIA,B44,1.1966) 463].
- [21] R. Wald, *General Relativity*, (Chicago University Press, Chicago, 1984).
- [22] C.M. Will, *Theory and experiment in gravitational physics*, 2nd ed. (Cambridge University Press, Cambridge, 1993); *Living Rev. Rel.* **4**, 4 (2001).
- [23] I. Chamblin, S. Hawking and H.S. Reall, *Phys. Rev. D* **61**, 065007 (2000).

- [24] R. Gregory, *Class. Quant. Grav.* **17**, L125 (2000).
- [25] R.C. Myers and M.J. Perry, *Ann. Phys.* **172**, 304 (1986).
- [26] L.A. Gergely, N. Pidokrajt and S. Winitzki, “Thermodynamics of tidal charged black holes,” arXiv:0811.1548 [gr-qc].
- [27] R. Casadio, S. Fabi and B. Harms, *Phys. Rev. D* **80**, 084036 (2009).